TISSUE ENGINEERING
Volume 12, Number 6, 2006

Quantifying the Directional Parameter of Structural Anisotropy in Porous Media

MARTIN Y.M. CHIANG, Ph.D., XIANFENG WANG, Ph.D., FORREST A. LANDIS, Ph.D., JOY DUNKERS, Ph.D., and CHAD R. SNYDER, Ph.D.

ABSTRACT

A new method has been developed to define the directional parameter and characterize the structural anisotropy of a highly porous structure with extensive pore interconnectivity and surface area, such as scaffolds in tissue engineering. This new method called intercept segment deviation (ISD) was validated through the comparison of structural anisotropy from ISD measurements with mechanical anisotropy from finite-element stress analysis. This was carried out on a generated two-dimensional (2D) image of a two-phase material and a real three-dimensional (3D) image of a tissue scaffold. The effect of tissue regeneration and scaffold degradation on the anisotropy of the scaffold was discussed. The performance of other methods for quantification of the directional parameter was also assessed. The results indicate that the structural anisotropy obtained from this new method conforms to the actual mechanical anisotropy and provides a better prediction of the material orientation than the other methods for the 2D and 3D images studied.

INTRODUCTION

IT IS WIDELY ACCEPTED that porosity and material architecture are highly relevant to the mechanical behavior of porous materials,[1–3] such as tissue engineering scaffolds. These porous materials usually have structural (or architectural) anisotropy that is related directly to the mechanical and functional anisotropies.[4–7] Much effort has been undertaken to formulate the relationship between architecture and mechanics to predict mechanical (elastic) anisotropy from structural anisotropy.[8–17] A successful formulation, in conjunction with other parameters, would enable prediction of the mechanical and physical properties of porous materials and tailor these materials to meet certain criteria for designer materials. It has been recognized that the structural integrity, mechanical influence, and physical properties are important factors regulating the cellular response in the scaffold.[18,19] In addition, knowledge of the structural anisotropy in advance from material images can facilitate experimental tests to determine the independent material constants needed for the macroscopic stress–strain relationships. Moreover, mechanical or physical properties (*e.g.*, the elastic constants, tortuosity or permeability) of the porous media can be predicted along the principal directions of material images. In this study, we develop a method to assess the structural anisotropy of tissue engineering scaffolds, which usually have interconnected channel-shaped pores rather than isolated cavities to guide cell growth and proliferation in three dimensions. One of the challenging issues in developing such a quantification technique is the complex microstructural topologies of biomaterial scaffolds. Moreover, comparisons to the prediction of structural anisotropy with other methods, which have been traditionally used for characterizing trabecular bone architectures, are also discussed in the study.

The characterization of structural anisotropy (or material orientation) in porous media has largely relied on deriving global measurement of intercept segments (as a directional parameter), which occur at the intersection of test lines and the boundary of material phase. Several mathematical constructs based on the intercept segment

Polymers Division, National Institute of Standards and Technology, Gaithersburg, Maryland.

have been provided in the literature for the measurement of a directional parameter, which can be used to evaluate the type and degree of structural anisotropy for porous media such as trabecular bone architectures.[8,16,20,21] The directional parameter is typically plotted in polar coordinates with respect to test lines in various angles, and the resulting curve is called a rose diagram (RD). The material is isotropic if the best fit to the diagram is a sphere (or a circle for a two-dimensional (2D) material image), and the material is anisotropic if the diagram differs from a sphere. Practically, no material is completely anisotropic; therefore, for the purpose of engineering analyses, a material is assumed to be orthotropic at most (not fully anisotropic, *i.e.*, no shear deformation would occur if the material is subjected to normal deformation in a principal direction).[22] In the orthotropic case,[1] material properties differ macroscopically in three mutually perpendicular directions (*i.e.*, has three mutually perpendicular planes of material symmetry), and the best fit to the RD should be an ellipsoid. The directions of these fit axes are principal directions. The ratio of the length of major to minor principal axes in the ellipsoid, defined as the degree of anisotropy (DA), expresses the departure from isotropy and can be correlated to the disorders of biological functions.[6] If the RD is a spheroid, then the medium is transversely isotropic and has a rotational symmetry with respect to one of the principal axes (i.e., has symmetry properties in the plane normal to that principal axis). More importantly, through the decomposition of the principal axes of the ellipsoid to eigenvalue–eigenvector pairs, one can correlate the structural anisotropy and the mechanical anisotropy to obtain those elastic properties needed for stress analysis.[15]

In this article a new method, named intercept segment deviation (ISD), is proposed to define the directional parameter for characterization of the structural anisotropy of highly interconnected tubular porous media with extensive surface area, such as tissue engineering scaffolds. The ISD method measures the standard deviation of intercept segments length, with respect to test lines in various angles, as the directional parameter. Conceptually, this directional parameter gives the degree of variability within the intercept segments about their mean intercept length and differentiates the material orientation from an idealized average material orientation. This new method is validated through the comparison of structural anisotropy from its measurements to mechanical anisotropy from finite element stress analysis (FEA). A generated 2D image of a two-phase material and a real three-dimensional (3D) image of a tissue scaffold are used to illustrate the comparisons over other methods. Also, the effects of porosity, individual phase geometry, and properties on the orientation of general two-phase materials have been systematically explored.

METHOD

Quantification of structural anisotropy

By applying a parallel array of test lines to a porous material image at angle α, intercepted line segments will arise at the intersection of the test lines with the boundary of the matrix phase. For example, a 2D material image having two phases (matrix and pores) is shown in Fig. 1. The intercept (fabric) length has been identified as a directional parameter of relevance to the structural anisotropy of the material, and several different methods to derive this parameter have been proposed for characterizing the structural anisotropy of the porous material.

The mean intercept length (MIL) method, developed early in 1945,[23] has been applied to quantify the directional parameter for the anisotropy of trabecular networks in bones.[21,25] The definition of MIL may be expressed as follows[9]:

$$MIL(\alpha) = \frac{\sum_{i=1}^{N(\alpha)} I_i(\alpha)}{N(\alpha)} \tag{1}$$

where $I_i(\alpha)$ corresponds to the intercept length of the ith line segment measured along the test lines drawn in the α direction, and $N(\alpha)$ represents the number of all the randomly intercepted segments in that direction. Measuring the MIL along test lines and drawing them in a polar plot with respect to α results in a RD. The total intercept length, $\sum_{i=1}^{N(\alpha)} I_i(\alpha)$ in Eq. (1), for all the directions remains a constant and physically is proportional to the volume–surface ratio of pores dispersed in a matrix.[24] Therefore, $N(\alpha)$ is the only variable in Eq. (1). If a sphere/isotropic phase interface exists, it is possible to obtain a spherical RD for an actually orthotropic medium (*i.e.*, anisotropic structures with isotropy at the surface do exist[26,27]). Consequently, this method determines the orientation of the interface rather than of the material itself, although these are often well related.

Several subsequent methods have been developed based on this "intercept length" concept for quantifying the structural anisotropy for trabecular architectures to overcome the potential problem associated with the MIL method, for example, the star volume distribution (SVD[8]), the star length distribution (SLD[15]), and the line fraction deviation (LFD[20]) methods. The SVD is a volume-based method and is evaluated using an array of parallel test lines as a function of each direction in space as:

$$SVD(\alpha) = \frac{\pi}{3} \frac{\sum_{i=1}^{N(\alpha)} I_i^4(\alpha)}{\sum_{i=1}^{N(\alpha)} I_i(\alpha)} \tag{2}$$

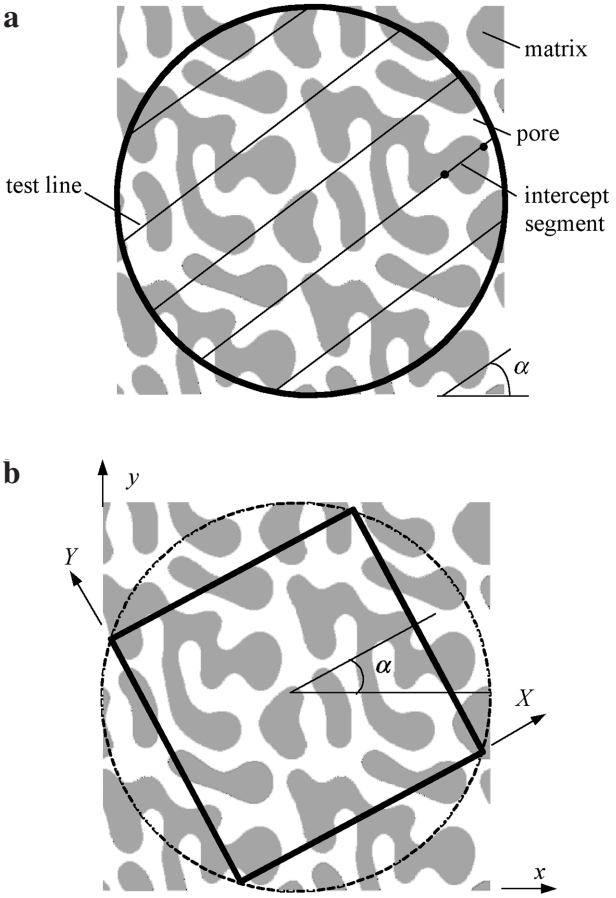

FIG. 1. Illustration of the measurement of intercept length in direction α for characterizing the structural anisotropy of a generated 2D image, a circle test region was chosen for the measurement **(a)**; a square test image was chosen and a uniform deformation is applied along the direction α for the measurement of mechanical anisotropy **(b)**.

The SLD method is similar to SVD, but lightly weights the fabric intercepts in calculating the anisotropy in porous media and is expressed as:

$$SLD(\alpha) = \frac{\sum_{i=1}^{N(\alpha)} I_i^2(\alpha)}{\sum_{i=1}^{N(\alpha)} I_i(\alpha)} \tag{3}$$

A point grid algorithm for calculating the SVD and SLD was also presented in the literature,[16] in which it was concluded that these methods provide marginally better predictions of the mechanical anisotropy directions of cancellous bone than the MIL method.

Besides the methods listed above, the LFD method was developed and compared with MIL for measuring orientation of trabecular bone structures.[20] It was shown that the LFD method, which determines the standard deviation of the fraction of the intercept length under an individual test line in the α direction, is more sensitive to anisotropy than the MIL technique. To the best of our knowledge, no explicit formulation in stereological terms is available in the literature. Therefore, we present a mathematical expression for the LFD method according to our understanding of the original notion in the literature as:

$$LFD(\alpha) = \sqrt{\frac{\sum_{j=1}^{M(\alpha)} (J_j(\alpha) - \bar{J}(\alpha))^2}{M(\alpha)}} \tag{4}$$

where $M(\alpha)$ is the number of total test lines in the direction α, and $J_j(\alpha)$ corresponds to the fraction of the intercept lengths for the jth test line. $J(\alpha)$ is the mean value of $J_j(\alpha)$'s with respect to $M(\alpha)$:

$$\bar{J}(\alpha) = \frac{\sum_{j=1}^{M(\alpha)} J_j(\alpha)}{M(\alpha)} \tag{5}$$

We propose a new approach called the ISD method, unlike the LFD method, which takes into account the deviation of each intercept segment from the mean value of total segment lengths in a test line direction, and is defined as:

$$ISD(\alpha) = \sqrt{\frac{\sum_{i=1}^{N(\alpha)} (I_i(\alpha) = \bar{I}(\alpha))^2}{N(\alpha)}} \tag{6}$$

and

$$\bar{I}(\alpha) = \sqrt{\frac{\sum_{i=1}^{N(\alpha)} I_i(\alpha)}{N(\alpha)}} \tag{7}$$

Mathematically, this method better reflects the degree of variability within the intercept segments than the LFD method and, physically, gives the variation of phase interface from an idealized sphere/isotropic phase interface.

In this study, two images were analyzed using the MIL, SVD, SLD, LFD, and ISD methods. The resulting RDs were compared with the mechanically determined anisotropy (which will be discussed later). One of the images is a generated 2D microstructure from a phase separation of polymer blends described by the Cahn-Hilliard-Cook model, which is an equation for phase separation.[28,29] In this 2D material image, one of the material phases is set to mimic pores and the porosity is 0.5. Another image to be examined is a 3D representation of the microstructure from x-ray tomography of a tissue scaffold with a porosity of 0.45. A rotating pixel and coordinate transformation scheme, where each pixel in the test region (*e.g.*, Fig. 1a) was locally rotated to the test line direction, was adopted as suggested in the literature to facilitate the accurate measurement of the directional parameter.[20] Also, it is worthwhile to note that in order to avoid an orientation preference, we took a circular or spherical test region during the evaluation of the directional parameter (Fig.

1a). This keeps the porosity constant through the calculation of the parameter in all the orientations concerned. In addition to the specific 2D and 3D cases shown in Figs. 1 and 2, we also applied the ISD method to different 3D digital images of scaffolds with porosities ranging from ca. 0.3 to 0.55, to demonstrate the universality of the new methodology in characterizing the material anisotropy.

Quantification of mechanical anisotropy

A major requirement for the relationship between structure and mechanics should be the ability to predict mechanical anisotropy from architectural anisotropy. Therefore, numerical simulations of the elastic mechanical tests of porous media, using large-scale finite element models generated from the 2D and 3D images, have been performed to validate the aforementioned methods for quantifying the structural anisotropy. In order to obtain the dependency of the elastic properties on the test direction, square and cubic test regions at each particular test direction (α) were chosen from the original 2D (for example, see Fig. 1b) and 3D images, respectively. By taking the test region for different angles and applying various mechanical constraints and virtual deformation along the angles, an elastic modulus as a function of test direction can be constructed (a RD for mechanical anisotropy).

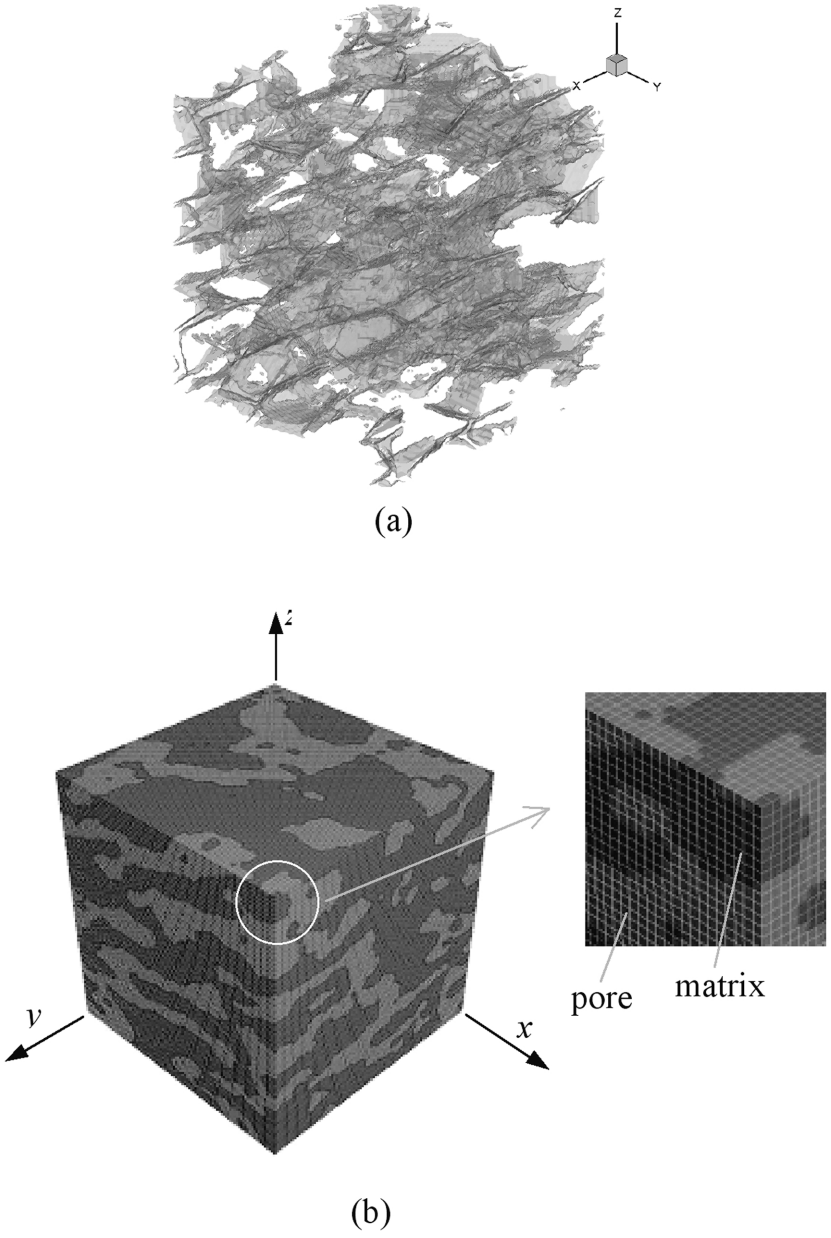

FIG. 2. View of the porous phase of a real 3D porous medium (**a**); 3D finite element model for the measurement of mechanical anisotropy (**b**). (Color images are available at <www.liebertpub.com/ten>.)

The commercial finite element program, ABAQUS,[30] was used to simulate the mechanical test. The porous material was modeled as a two-phase material system in the finite element analysis based on the configurations shown in Figs. 1b and 2. The matrix phase of the porous media was assumed to be a homogeneous, isotropic, and linear elastic continuum. In 2D analysis, a plane stress condition was adopted. Finite element meshes were generated using four-node and three-node isoparametric continuum elements provided by the program. In 3D analyses, finite element meshes were automatically generated using a voxel-based scheme developed in our lab. This scheme converts a high-resolution image into meshes with hexahedral elements. All elements in these meshes are identical and have the same dimensions as the voxels in the image. Millions of degrees of freedom are contained in the micro-finite element model for the material image studied here.

RESULTS AND DISCUSSION

To assess the aforementioned methods on the accuracy of predicted structural anisotropy, we first performed finite element analyses to establish the mechanical anisotropy for the 2D and 3D porous images in Figs. 1 and 2, respectively. For the 2D image, the dotted line in Fig. 3a is the best elliptical fit to the RD of the modulus as a function of test direction. This elliptical fit implies that the two-phase material studied is orthotropic, having three mutually perpendicular planes of material symmetry. The directions of these fit axes are principal directions (*i.e.*, no shear deformation would occur if the material is subjected to normal deformation in a principal direction). For the purpose of illustration, the RD of the mechanical anisotropy of the 3D image was decomposed into three independent RDs in the planes with respect to the original reference coordinates of the image in Fig. 2. It was found that the principal axes for the 3D image were nearly identical to the original reference axes (x, y, and z). This is also why the longest axes of those three decomposed RDs (Fig. 3b) lie near 0° or 90°.

For the finite element analysis of mechanical response, the test region rotated with the test direction α (i.e., Fig. 2). As a result, the porosity of the image in each square test region could be different due to the random distribution of the pores in the material image. Because the mechanical response would be affected not only by the microstructure but also the porosity, it was worthwhile to examine the variation of the porosity in the test region as a function of the test direction. The result in Fig. 4 indicates that the deviation from the original porosity (= 0.5) is minimal, and one can conclude that the resulting change in the elastic modulus shown in Fig. 3 is solely attributed to the microstructural change in the test direction rather than the porosity.

For a more general two-phase material case, the effect of the stiffness ratio on the type and degree of mechanical anisotropy has been examined. The stiffness ratio is defined as E_1/E_2, where E_1 and E_2 are the elastic moduli of the phase 1 and phase 2 materials, respectively. For each test direction, mechanical tests have been performed with the stiffness ratio varying from 1 to 10^4, and the 2D image in Fig. 1 has been used for the mechanical test due to simplicity. Subsequently, RDs from the mechanical tests as a function of the stiffness ratio can be constructed. It is found that all the RDs have a reasonably good elliptic fit and their principal directions, as expected, remain unchanged, while the

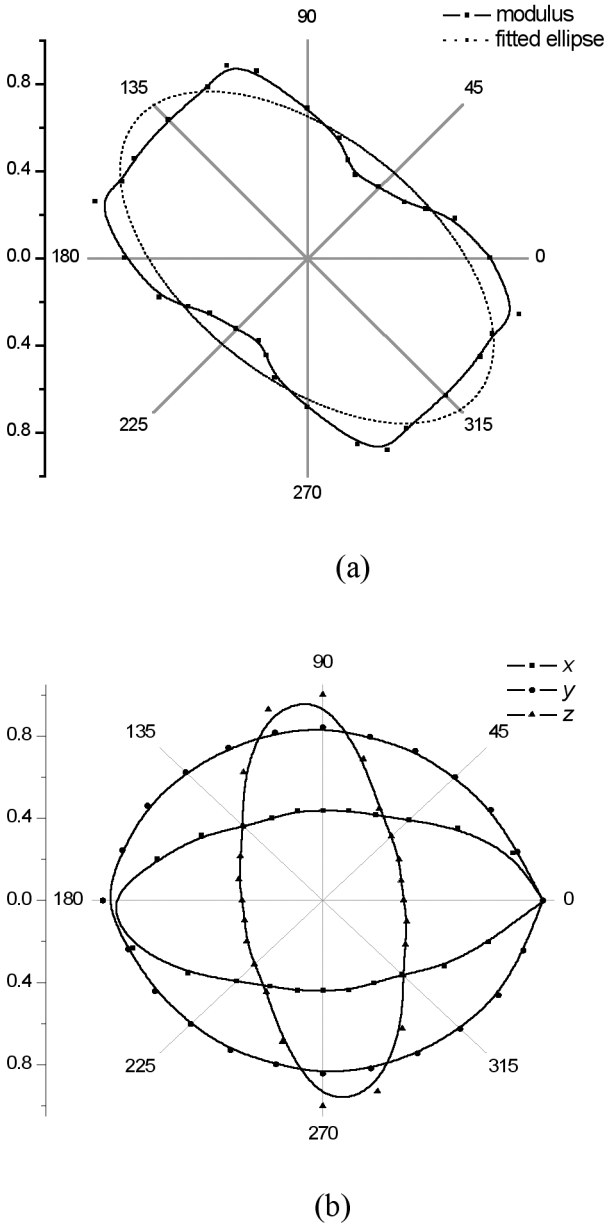

FIG. 3. Rose diagrams obtained from the normalized modulus as a function of test direction for images shown in Fig. 2. A rose diagram for the 2D image (**a**); decomposed rose diagrams for the 3D image (**b**).

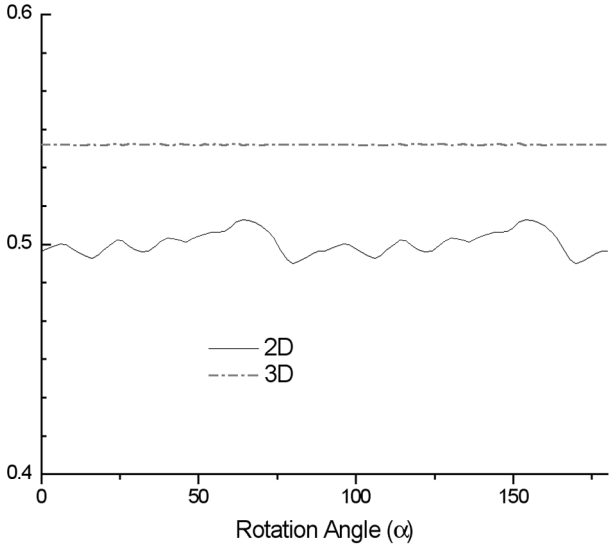

FIG. 4. The variation of matrix concentration with rotation angle of test images for 2D and 3D porous media.

stiffness of the materials in the phases 1 and 2 changes (Fig. 5). However, the mechanical DA is affected, which increases with the increase of the stiffness ratio and tends to be a determining value when the material has two strong-contrast phases (e.g., E_2 approaches zero, which corresponds to pores). The results in Fig. 5 indicate that the principal directions of the two-phase materials, if they exist, are only functions of geometry and the spatial arrangement (microstructure) of the two phases. Conversely, the mechanical DA of the two-phase material is dependent not only on the microstructure, but also on the stiffness ratio of the constituents. In tissue engineering scaffolds, this implies that the existence of *regenerated tissue (or cells) in pores does not alter the anisotropy of the scaffold, but relative rigidity between the scaffold material and the regenerated tissue may alter the DA of the scaffold.* Practically, the rigidity of scaffold material is much more than that of the regenerated tissue, so the mechanical DA of the scaffold with filled regenerated tissues should be the same because it is an unfilled porous medium. Also, the tissue growth into a porous scaffold would represent a tri-phase material. The aforementioned statements should be adequate because the pores

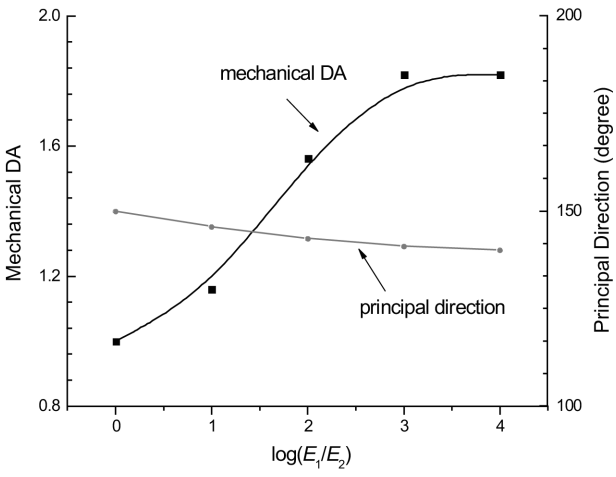

FIG. 5. The mechanical DA and principal direction as a function of constituent properties of 2D image shown in Fig. 1.

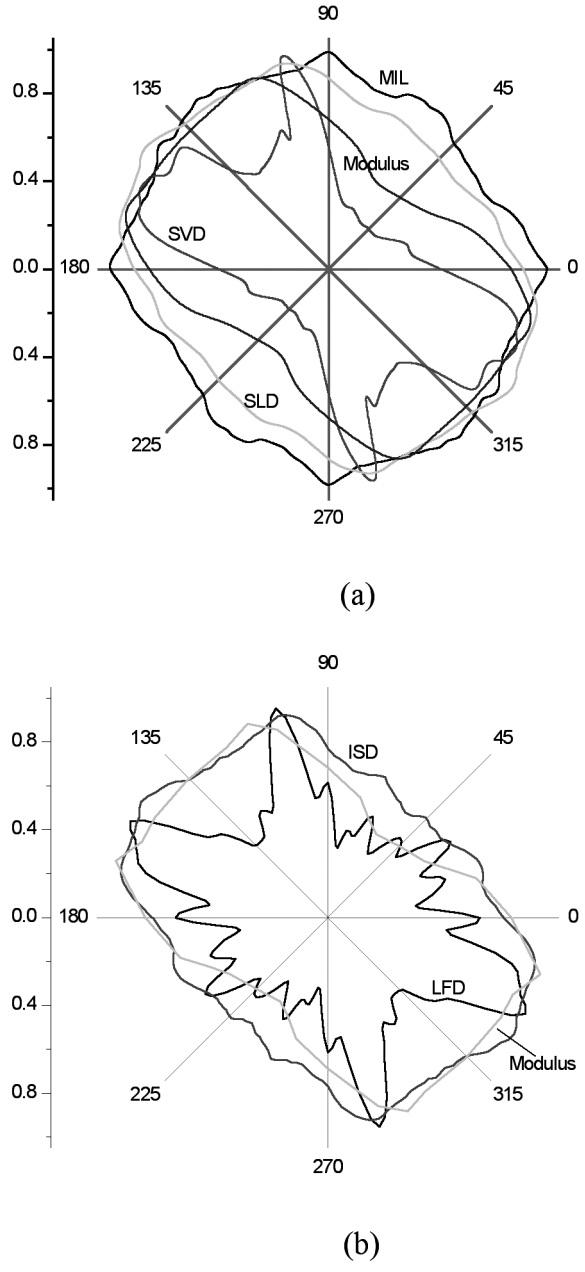

FIG. 6. Comparisons of rose diagrams obtained from different methods with that obtained from FEA for a 2D porous medium shown in Fig. 1.

and materials grown in the pores can be treated, together, as an effective one-phase material since they are soft matters.

Fig. 6 presents the RDs for structural anisotropy obtained from the MIL, SVD, SLD, LFD, and newly developed ISD methods for the 2D image in Fig. 1. Also, for comparison, shown in the figure is the RD for the mechanical anisotropy obtained from the finite element analysis. Based on the similarity of the structural and the mechanical RDs, one can assume that the proposed ISD method has greater sensitivity to the material orientations than the other methods studied and can well predict the principal mechanical directions. Also, the RD obtained from the ISD method can attain a best elliptic fit (Fig. 6), which indicates that the material images are considered to be orthotropic. In addition, this result supports the assumption that the *mechanical orientations are aligned with the fabric orientations*.

Fig. 7 gives the comparison between the projected RDs, in three orthogonal planes, obtained from the FEA and the proposed ISD method for the 3D image in Fig. 2. The 3D RDs of FEA and ISD method are spheroids (not shown here), which result in ellipses identical in shape after the projection (Figs 7a and 7c). This indicates that the image in Fig. 2 macroscopically behaves as transversely isotropic material, which has a rotational symmetry with respect to the z axes. This information reveals that only five independent material constants need to be

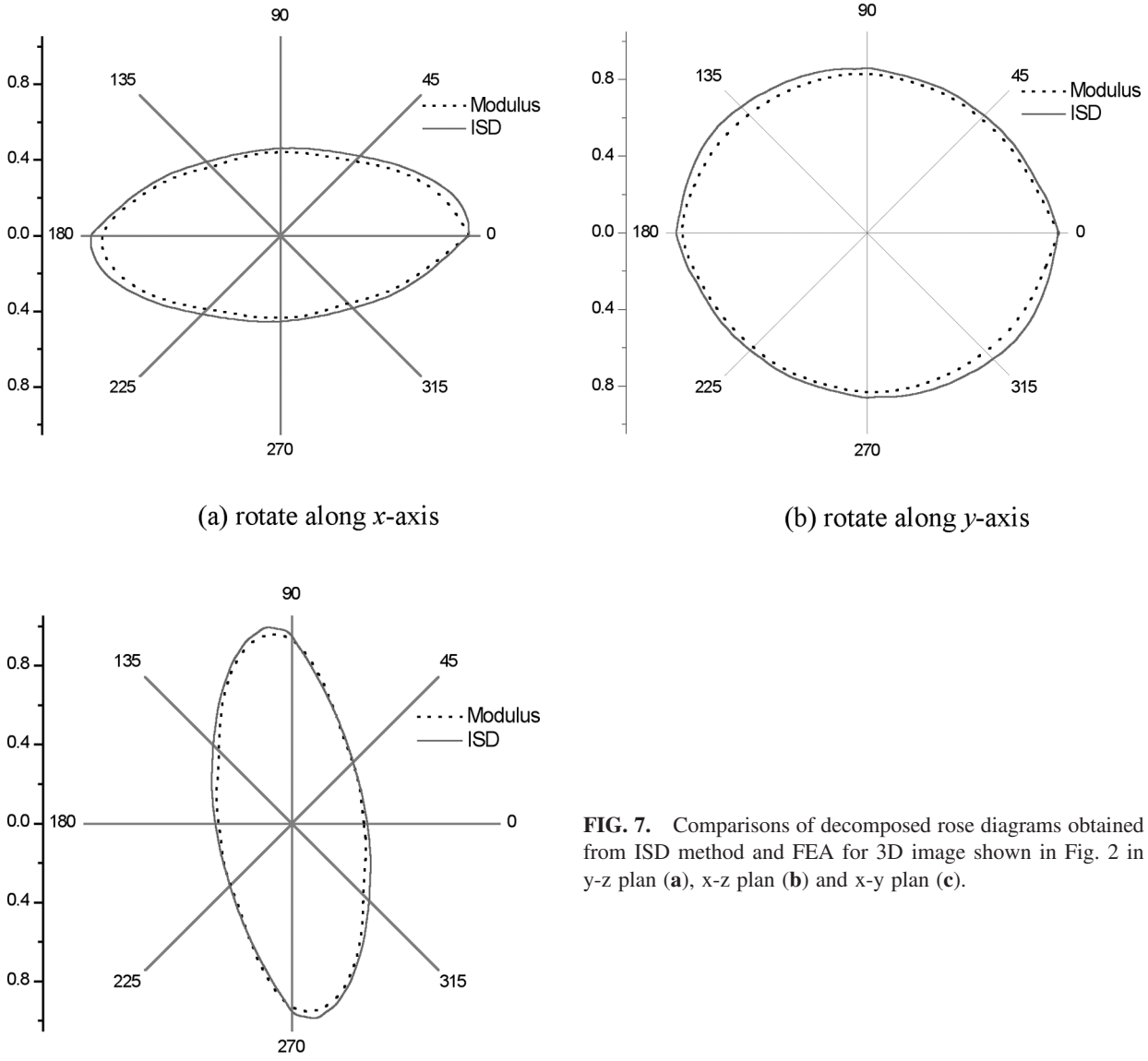

FIG. 7. Comparisons of decomposed rose diagrams obtained from ISD method and FEA for 3D image shown in Fig. 2 in y-z plan (**a**), x-z plan (**b**) and x-y plan (**c**).

determined for the stress–strain relations in coordinates aligned with principal directions. For the purpose of clarity, the RDs obtained from other methods are not shown here. Overall, the results in Figs. 6 and 7 indicate that the ISD method gives accurate predictions in characterizing the structural anisotropy.

In order to examine the relationship of the pore shape and size to the structural anisotropy, one can keep the pore architecture constant (pore shape and connectivity) while changing the pore size (consequently, changing the porosity). The images in Fig. 8 were produced based on the image in Fig. 1 (porosity = 0.5) by either expanding or contracting the matrix–pore interface uniformly. This also mimics an ideal reality in tissue engineering where the tissue regeneration and scaffold degradation take place simultaneously. For example, Fig. 8a can represent a structure starting from the scaffold alone (matrix volume fraction = 0.6, porosity = 0.4), to a composite structure of degrading scaffold and regenerating tissue (matrix volume fraction = 0.5 to 0.2; i.e., Fig. 8b–e), to almost regenerated tissue (matrix volume fraction = 0.1; i.e., Fig. 8f). Some of the RDs obtained from the ISD measurement corresponding to these microstructures are depicted in Fig. 9. The result in the figure indicates that initially, the shape and the orientation of those RDs remain basically unchanged, and a best fit of ellipse for each diagram can be found. This suggests that the type of anisotropy of the structure remains orthotropic during the processes of matrix contraction (*i.e.*, scaffold degradation) or pore expansion (*i.e.*, tissue regeneration). Also, the diagram approaches a circle when the scaffold concentration reduces to 0.1.

Fig. 10 shows the principal direction and the structural DA as a function of matrix volume fraction. During the degradation of matrix volume fraction from 0.6 to 0.2, the principal direction and the DA are roughly independent of the porosity while the shape and arrangement of the pore architecture remain unchanged. This result shows that the porosity and architectural orientation are independent parameters for quantitatively describing the mechanical and physical properties of porous media. For the further matrix degradation in Fig. 10 (*i.e.*, the matrix volume fraction from 0.2 to 0), the DA tends to be 1.0, because the structure approaches isotropy. Also, at this stage, the RD is close to a circle, and consequently, the principal direction becomes singular (no preference of the material orientation).

Fig. 11 gives the variation of the DA obtained using the ISD and MIL methods on the images of the porous engineering scaffold. Each datum in the figure corresponds to a mean value of DAs obtained from analyzing 4 to 6 cubic portions of the entire specimen. These cubic images were collected from different locations within the same specimen. It should be noted that regardless of the positions where these 3D sample cubes were taken, the porosity was essentially constant (the variation in porosity was less than 1%). This was done to keep the porosity constant, whereas the microstructure was various. From the value of the error bars in Fig. 11, which is the standard deviation, one can see that the DA does not change significantly for the images from the same specimen (*i.e.*, the same porosity). This is because each specimen can be treated as macroscopically homogenous. Also, for this engineering scaffold, the DA obtained from both methods reaches its highest value at a porosity of approximately 45%. There is a discrepancy between the DAs evaluated from the ISD and MIL methods. In the case of the ISD method, when the porosity becomes ei-

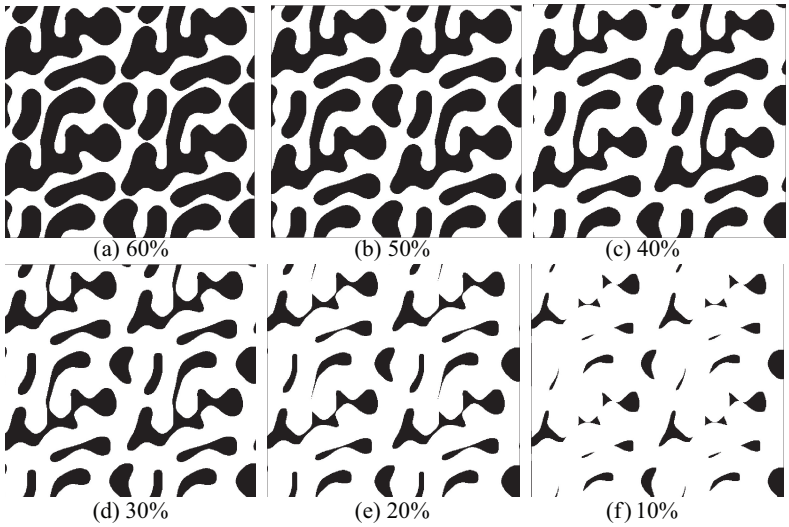

FIG. 8. 2D image with different matrix concentration while maintaining matrix shape unchanged (white: pore; black: matrix).

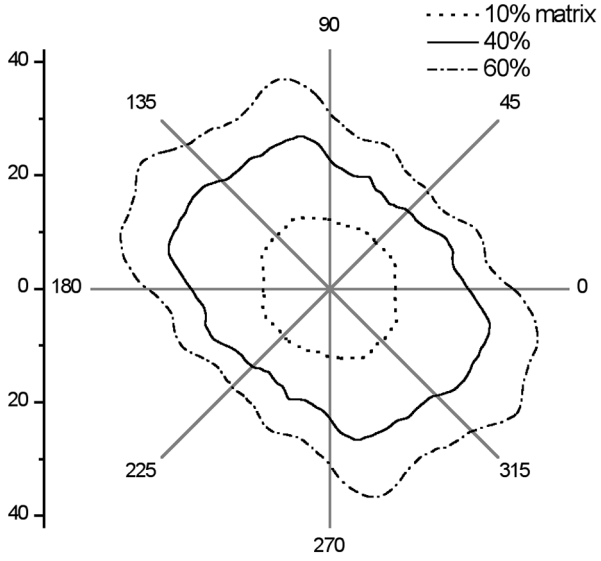

FIG. 9. Structural anisotropy obtained from ISD method for some of 2D images in Fig. 8.

ther lower or higher than 45%, the DA tends towards to unity. This agrees with the physical situation because the material becomes more isotropic (*i.e.*, a one-phase material). However, the DAs analyzed using the MIL method, which has been widely used to quantify the anisotropy of trabecular networks in bones, do not agree with the physical situation for the engineering scaffold studied. In conjunction with the results in Fig. 5 (the independence of the principal direction on the stiffness ratio), Fig. 9, and Fig. 10, the result in Fig. 11 suggests that the proposed ISD method can be extended to any general two-phase materials for quantifying the directional parameter.

CONCLUSION

In this study, we have developed a new fabric-based scheme called the intercept segment deviation (ISD) method, which takes into account the local variation of the orientation, to quantify the directional parameter that characterizes the structural anisotropy of highly porous medium with complex microstructural topologies. The structural anisotropy calculated from this method agrees well with the actual mechanical anisotropy and performs better than any of the other methods studied. The study has presented the interrelationship of the geometry, spatial arrangement, and individual constituent properties on the macroscopic mechanical response of the two-phase materials. Also, we conclude that the concentration and structural anisotropy are two independent microstructural factors of relevance to the mechanical properties of two-phase materials, although the mechanical properties might be more related to the concentration. In addition, the degree of anisotropy obtained using the directional parameter from image analysis is only good for porous media or media with strong-contrast phases. The results presented here can facilitate the optimal design and fabrication of scaffold used in medicine and in tissue engineering. Finally, although the current study is based on use of a restricted set of microstructure images, the method can be extended to any general two-phase materials.

REFERENCES

1. Lin, A.S.P., Barrows, T.H., Cartmell, S.H., and Guldberg, R.E. Microarchitectural and mechanical characterization of

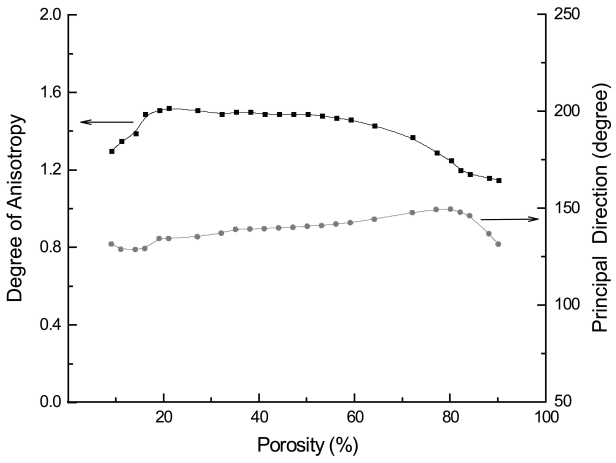

FIG. 10. The variation of principal direction and DA with porosity for 2D image in Fig. 8.

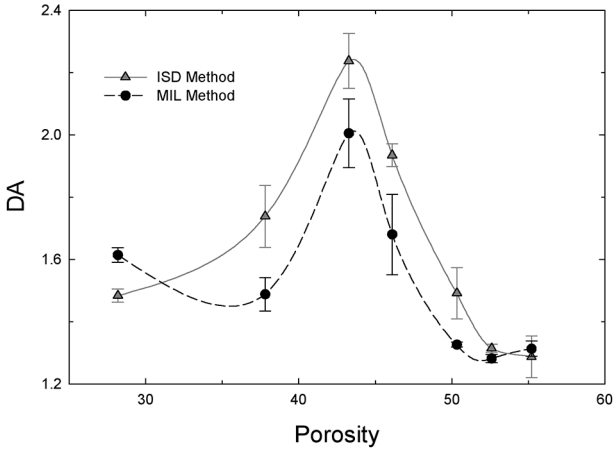

FIG. 11. The variation of the DA obtained using the ISD and MIL methods on the images of the porous engineering scaffold. The error bar is the standard deviation.

oriented porous polymer scaffolds. Biomaterials **24,** 481, 2003.
2. Pothuaud, L., Van Rietbergen, B., Mosekilde, L., Beuf, O., Levitz, P., Benhamou, C.L., and Majumdar, S. Combination of topological parameters and bone volume fraction better predicts the mechanical properties of trabecular bone. J. Biomech. **35,** 1091, 2002.
3. Roberts, A.P. and Garboczi, E.J. Computation of the linear elastic properties of random porous materials with a wide variety of microstructure. Proceedings of the Royal Society of London Series A—mathematical physical and engineering sciences **458,** 1033, 2002.
4. Slivka, M.A., Leatherbury, N.C., Kieswetter, K., and Niederauer, G.G. Porous, resorbable, fiber-reinforced scaffolds tailored for articular cartilage repair. Tissue Eng. **7,** 767, 2001.
5. Krishnan, L., Weiss, J.A., Wessman, M.D., and Hoying, J.B., Design and application of a test system for viscoelastic characterization of collagen gels. Tissue Eng. **10,** 241, 2004.
6. Polikeit, A., Nolte, L.P., and Ferguson, S.J. Simulated influence of osteoporosis and disc degeneration on the load transfer in a lumbar functional spinal unit. J. Biomech. **37,** 1061, 2004.
7. Muller, R., and Ruegsegger, P. Analysis of mechanical properties of cancellous bone under conditions of simulated bone atrophy. J. Biomech. **29,** 1053, 1996.
8. Cruz-Orive, L.M., Karlsson, L.M., Larsen, S.E., and Wainschtein, F. Characterizing anisotropy: A new concept. Micron Microsc. Acta **23,** 75, 1992.
9. Inglis, D., and Pietruszczak, S. Characterization of anisotropy in porous media by means of linear intercept measurements. Int. J. Solids Structures **40,** 1243, 2003.
10. Kanatani, K. Procedures for stereological estimation of structural anisotropy. Int. J. Eng. Sci. **23,** 587, 1985.
11. Oda, M. Initial fabrics and their relation to mechanical properties of granular materials. Soils Foundations **12,** 7, 1972.
12. Odgaard, A., Jensen, E.B., and Gundersen, H.J.G. Estimation of structural anisotropy based on volume orientation. A new concept. J. Microsc. **157,** 149, 1990.
13. Pietruszczak, S., and Mroz, Z. On failure criteria for anisotropic cohesive-frictional materials. Int. J. Numer. Analyt. Methods Geomech. **25,** 509, 2001.
14. Odgaard, A. Three-dimensional methods for quantification of cancellous bone architecture. Bone **20,** 315, 1997.
15. Smit, T.H., Schneider, E., and Odgaard, A. Star length distribution: a volume-based concept for the characterization of structural anisotropy. J. Microsc.-Oxford **191,** 249, 1998.
16. Odgaard, A., Kabel, J., vanRietbergen, B., Dalstra, M., and Huiskes, R. Fabric and elastic principal directions of cancellous bone are closely related. J. Biomech. **30,** 487, 1997.
17. Van Lenthe, G.H., and Huiskes, R. How morphology predicts mechanical properties of trabecular structures depends on intra-specimen trabecular thickness variations. J. Biomech. **35,** 1191, 2002.
18. Yang, S.F., Leong, K.F., Du, Z.H., and Chua, C.K. The design of scaffolds for use in tissue engineering. Part 1. Traditional factors. Tissue Eng. **7,** 679, 2001.
19. Detamore, M.S., and Athanasiou, K.A. Motivation, characterization, and strategy for tissue engineering the temporomandibular joint disc. Tissue Eng. **9,** 1065, 2003.
20. Geraets, W.G.M. Comparison of two methods for measuring orientation. Bone **23,** 383, 1998.
21. Whitehouse, W.J. The quantitative morphology of anisotropic trabecular bone. J. Microsc.-Oxford **101,** 153, 1974.
22. Miller, Z., Fuchs, M.B., and Arcan, M. Trabecular bone adaptation with an orthotropic material model. J. Biomech. **35,** 247, 2002.
23. Keaveny, T.M., and Hayes, W.C. A 20-year perspective on the mechanical properties of trabecular bone. J. Biomech. Engin. Trans. ASME **115,** 534, 1993.
24. Tomkeieff, S.I. Linear intercepts, areas and volumes. Nature **155,** 107, 1945.
25. Harrigan, T.P., and Mann, R.W. Characterization of microstructural anisotropy in orthotropic materials using a 2nd rank tensor. J. Materials Sci. **19,** 761, 1984.
26. Fyhrie, D.P., Hollister, S.J., Schaffler, M.B., and Kimura, J. Structural transformations indistinguishable by point-count stereology. J. Biomech. **25,** 685, 1992.
27. Odgaard, A., Andersen, K., Ullerup, R., Frich, L.H., and Melsen, F. 3-Dimensional reconstruction of entire vertebral bodies. Bone **15,** 335, 1994.
28. Cahn, J.W., and Hilliard, J.E. Free energy of a nonuniform system I. Interfacial free energy. J. Chem. Physics **28,** 258, 1958.
29. Cook, H.E. Brownian motion in spinodal decomposition. Acta. Metall. **18,** 297, 1970.
30. ABAQUS Finite Element Analysis Code and Theory. Providence, RI: Hibbitt, Karlsson & Sorensen, Inc. 2002. (Certain commercial computer code is identified in this paper in order to specify adequately the analysis procedure. In no case does such identification imply recommendation or endorsement by the National Institute of Standards and Technology (NIST) nor does it imply that they are necessarily the best available for the purpose.)

Address reprint requests to:
Martin Y.M. Chiang, Ph.D.
Polymers Division
National Institute of Standards and Technology
Gaithersburg, MD 20899-8544

E-mail: martin.chiang@nist.gov